1. INTRODUCTION

1.1 Background of Study

It is with no doubt that, ever since reinforced concrete was first introduced to the world in the year 1849, tons of researches have been done to figure out its properties such as how much load can it withstand, how the reinforced concrete member behaves when certain amount of load is being enforced onto it, how adding other materials influence the strength of the reinforced concrete member, etc. These are all significant initiatives to not only strengthen the load capacity of reinforced concrete members, but also to be able to predict accurately how a reinforced concrete member will behave under different environment and loading conditions.

Malaysia currently practices Eurocode as the standard for structural design, with the structures (be it steel, concrete or reinforced concrete) designed according to the ultimate limit state. Ultimate limit state is when the maximum static load with high possibility of occurrence is imposed on the structure, the reinforced concrete member with a compressive strength that has been limited by a certain amount of safety factor will be able to withstand it [3]. This is to ensure that during the worst case scenario, where an uncommonly high load (that exceeds the designed strength of structure) with very low possibility of occurrence is being applied onto the structure, there is still a gap between the allowable designed stress and the actual yield stress of the structure.

However, as far as static load can go, there are still exceptions in structures that have to be designed to withstand dynamic loadings, from onshore buildings with exposure to high wind loads to offshore structures that has to withstand cyclic loadings caused by the wave and current.

1.2 Problem Statement

While the current popular design of structure according to ultimate limit state concept suffices to an extent to keep the structure safe, some reinforced concrete structures have to be designed more accurately for impact loads such as structures with high exposure to rockfalls or factories dealing with falling heavy loads [4]. This is to ensure a more precise evaluation of the structure against impact loads and to predict the failure probability.

Compared to other types of dynamic loading, impact loading is by far one of the cases with the most literature available on its study, from experimental works [5] to non-linear finite element analysis on the dynamic behavior of reinforced concrete beams [6]. Most researches in this field are done in order to enhance the general knowledge on the dynamic behavior of reinforced concrete members, especially on how it differs from the static behavior.

Apart from these researches, there are others that are done in an attempt to come up with simplified calculation methods to predict the dynamic response of reinforced concrete structures [2] [4] [5]. These are admirable initiatives, as the dynamic behaviors of reinforced concrete is currently heavily dependent on performing numerous simulations and experimental works. However, as far as the author comprehends, there are still insufficient evidences on the results obtained to confirm their reliability.

1.3 Objectives

The objectives of this project is to perform a parametric study on the dynamic behavior of reinforced concrete beam when subjected to impact load at its mid-span.

1.4 Scope of Study

In this research, the impact load acting on the beam model is simulated by using the Falling Weight Impact Loading Test, where a drop weight is allowed to free-fall at a certain height unto the mid-span of the beam model. The loading rate of the drop weight is controlled by performing the test using a specific mass of drop weight and a fixed velocity at contact between the drop weight and the surface of the beam.

For the parametric study of the structural behavior of the beam, the parameters that will be monitored include the longitudinal reinforcement ratio, shear reinforcement ratio and the shear span to depth (a/d) ratio in relation to the drop weight mass and velocity at contact.

Among the outcomes expected include the monitoring of the maximum deflection, the impact force at the mid-span of the beam and the reaction forces at the bottom supports of the beam model..

2. LITERATURE REVIEW

2.1 Parametric Study

Over the past few decades, several studies have been published in the area of reinforced concrete members subjected to dynamic loading, which is often generated by impact. A general trend towards an increase in the absorbed energy as the loading rate increases has been reported from these tests. For example, Banthia and Mindess [7] has done experimental work on plain concrete, and discovered that at higher stressing rates, plain concrete beams show higher impact strengths and also higher fracture energies, thus concluding that concrete is a material that is very sensitive to strain rate. However, the behavior of a structural component under impact loading seems to exhibit two response phases: an overall response when under low loading rate and a local response due to the high stress wave that occurs at the loading point during a very short period after impact (high loading rate) [1] [2] [8].

Fujikake et al. [8] carried out a drop-weight impact test of twelve specimens of RC beams with different impact velocities due to different drop heights, ranging from 1.71 m/s to 6.86 m/s. The influence of drop height and varying longitudinal reinforcement ratio on the impact responses of the RC beams were investigated. Jiang et al. [9] performed a Finite Element Analysis on the exact beams [8], and was able to match his results with Fujikake's experimental ones, proving that both results are accurate and quite ideal. Apart from that, Adhikary et al. [5] carried out concentrated loading with varying rates ranging from 0.0004 m/s for static load test to 2 m/s for impact load test, where the ultimate load carrying capacity, stiffness and energy absorption of RC beams were monitored. The results from all the aforementioned papers indicated that under static and low loading rates, the RC beam undergoes a flexural failure as the stress are distributed almost uniformly from the impact point to the tension side of the support. However, under high loading rates, the beams under impact load exhibited localized failure, and the flexural cracks do not reach the supports at both sides. Therefore, it shows that high loading rates significantly

influence the behavior of reinforced concrete structural elements with increase in resistance and change in failure mode of the structural members.

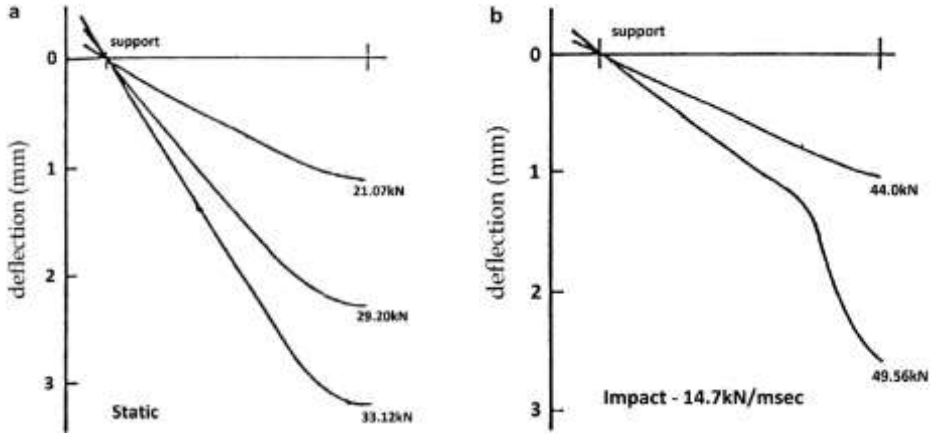

FIGURE 2.1.1. Deflected shapes predicted for RC beams under (a) static loading and (b) impact loading [1]

The aspect ratio of a structural member is defined as the ratio of shear span to the depth (a/d) of the member, where the shear span refers to the point of loading on the beam to the bottom supports, and it is able to influence the probable failure mode of the structural members, too. In general, it has been accepted that the aspect ratio of 2 - 2.5 is the critical ratio for static loading [11] [20], where values with aspect ratio lower than this will result in shear failure on beams whereas beams higher aspect ratios exhibit flexural failure. This phenomenon is tested by Perdomo et al. [10] by performing an experimental analysis using Digital Image Correlation (DIC) in order to determine the resistance and deformation capacity of structural members to predict their inelastic responses. The study has shown that for beams and columns of large aspect ratios, the most important effect is bending or deflection. But with its reduction, shear stresses become progressively more dominant. This finding was supported by Sharma and Ozbolt [11], who carried out a numerical study on a rectangular RC cantilever beam with a varying aspect ratio of 2, 4, 6 and 8, all subjected to low to high drift rates. It was found that, at the highest drift rate, for beam with aspect ratio of 2, shear failure is observed along with shear-compression cracks. As the aspect ratio

increases, flexure-shear cracks accompanied by cover peeling leads to the failure of the beams. These findings are only applicable for beams with longitudinal reinforcement ratio of 0.5% and above, as the failure mode of the beam is mainly flexural at low longitudinal reinforcement ratios regardless of the a/d ratio [20].

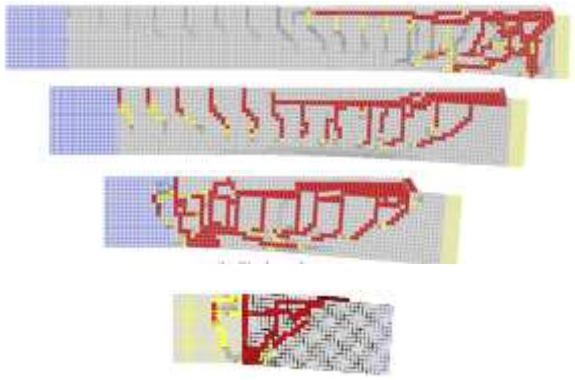

FIGURE 2.1.2. Failure modes obtained from beams of aspect ratio 8,6,4 and 2 respectively, under high loading rate [11]

Apart from testing on the influences of aspect ratio on the dynamic behavior of beam, Ozbolt and Sharma [12] also performed a numerical simulation of RC beams with different shear reinforcements. Based on their numerical results obtained, they have reached a conclusion that the static reaction depends largely on the amount of shear reinforcement and whether the beams are designed to be shear or flexural critical whereas the dynamic reactions of the beams were found to be independent of the amount of shear reinforcement as well as whether the beam is flexural critical or shear critical. As long as there are sufficient shear reinforcements, well distributed cracks tend to form in the beams. This conclusion is agreeable with Saatci and Vecchio's [22] findings. However, Saatci and Vecchio [22] added that even though the shear reinforcement does not affect the failure mode much, it is observed that specimens with higher shear capacity has higher impact resistance force and is able to absorb more energy, similar to the findings of varying longitudinal reinforcement ratio.

In order to be able to predict the behavior of reinforced concrete beam members more accurately without having to go through numerous simulations and experimental works, a vast number of attempts to generate empirical formulas regarding the dynamic behavior of beam have been done by various researches. For example, in their research, Adhikary et al. [5] came up with 3 empirical equations: a simplified equation to correlate the peak strain rate and loading rate in order to calculate the Dynamic Increase Factor (DIF) and two other empirical equations in terms of various parameters to predict the DIF of maximum resistance of RC under varying loading rates. Kishi and Mikami [4] had also came up with the empirical formulas for impact-resistant design, where the main focus is the prediction of the load-carrying capacity in relation to the maximum deflection and/or the residual deflection of the beam section. However, the empirical formulas generated by the above two researches have a few limitations of which governs the accuracy and sensitivity of the results obtained from the calculations, therefore more experimental investigations with a wider variation in parameters are required to be done to validate and improve the suggested empirical formulas.

In relation to aspect ratio and the resistivity of reinforced concrete beams under varying loading rates, Sharma and Ozbolt [11] found out that at an increase in loading rate, the tensile stresses experienced in the beam does not reach the support, in fact it is getting nearer to the applied load. The same thing was observed when the loading rate was fixed but the experiment was done with increasing aspect ratio, where even though the area of tensile stresses has increased relatively, the distance between the end of tensile stresses when it reaches the bottom surface of beam and the bottom support are getting further apart. This was visually observed by the crack patterns formed during the analysis. Sharma and Ozbolt deduced that this phenomenon is due to initial forces caused by the high loading rate, and it apparently has a higher influence on beams with larger aspect ratios compared to the ones with low aspect ratio. The same trend was observed by Cotsovos [2], who refers to it as the effective length of beam. He devised a simplified method for evaluating the load carrying capacity of

reinforced concrete beams when subjected to concentrated impact loading at their mid-span. This method links the enhancement of load-carrying capacity with the effective length of the beams.

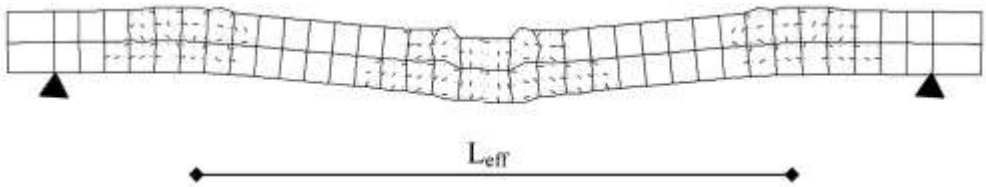

FIGURE 2.1.3. Deformed shape of the RC beam and crack patterns which develop along its length when subjected to concentrated high loading rate at its mid-span. [2]

The good correlation between the prediction of the proposed method, the numerical investigation and the experimental values from another research by Cotsovos [14] that carried out five test series on beams with same cross-sectional dimensions, span and similar reinforcement arrangements but different amount of longitudinal and transverse reinforcements, provides an indication of the validity of the method proposed.

2.2 Finite Element Analysis

The parametric study of the behavior of the beam under impact loading is to be carried out using Finite Element Method by using the software LS-DYNA. LS-DYNA is a highly non-linear, transient dynamic finite element analysis program which uses explicit time integration [13]. It provides numerous material models in its material library and various types of element formulations in its element library.

Since this software provides a vast number of material models, it is crucial to choose the most suitable ones in order to simulate the models as according to the actual experimental work accurately. For the study, the concrete beam is modelled using the material Concrete Damage Rel. 3 or MAT_072R3, also known as the K&C Concrete

Model. The default parameter of this model has been calibrated using a well characterized concrete with available uniaxial, biaxial, and triaxial test data in both tension and compression [16]. The input for this material keyword includes mass density of concrete, Poisson's ratio, unconfined compression strength and the defined effective strain-rate effects curve. The effective strain rate curve used in this study is extracted from Malvar's study [18] [21], where the dynamic increase factor (DIF) needed for high strain rate cases in terms of strain factor against time is considered.

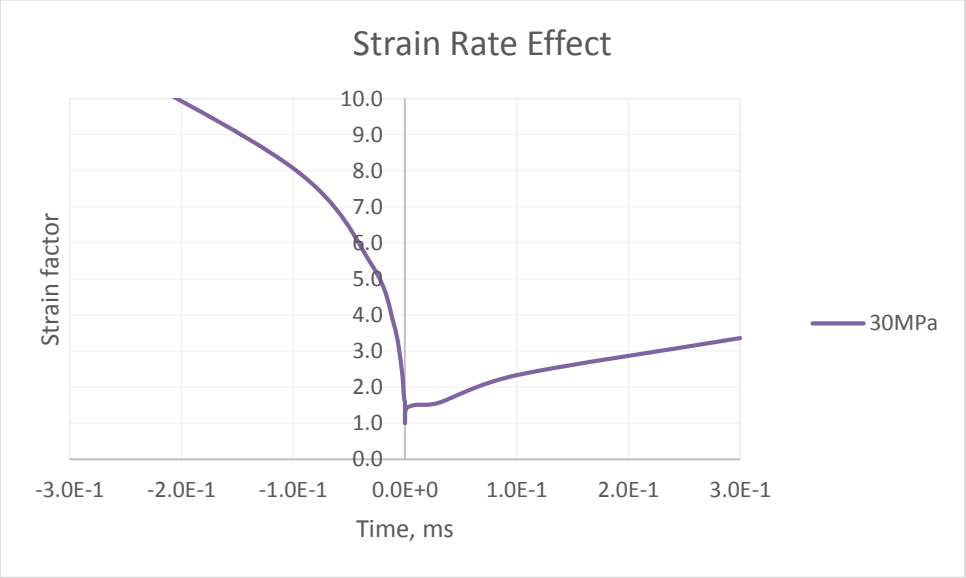

TABLE 2.2.1. DIF curve of concrete with strength 30 MPa.

The material properties of reinforcement steel bars for both longitudinal and also shear are inputted into the software through the keyword MAT_003-Plastic Kinematic. This model is suited to model isotropic and kinematic hardening plasticity with the option of including rate effects [13]. Among the inputs for this keyword are the mass density, Young's modulus, Poisson's ratio and yield strength of steel. The dynamic effects of strain rates are taken into account by scaling yield stress with the Cowper-Symonds model factor:

$$\frac{\sigma_d}{\sigma_s} = 1 + (\frac{\varepsilon}{C})^{\frac{1}{p}}$$

Where σ_d = dynamic yield stress, σ_s = static yield stress, ε = strain rate, and C,P = constants of Cowper-Symonds relation. The values of coefficient C and P for mild steel are given to be 40.4 and 5 respectively [19]. These values are used by several work [17] [15], including Gyliene and Ostasevicius [15] in their research, where they have successfully validated the FE model of orthogonal turning.

As stated before, material card MAT_072R3 is used for the beam model, as not only can it automatically generate parameters with only the compressive strength of concrete required as input, but it can accurately describe the material response for standard tests as uniaxial extension and compression. However, comparing to other material cards such as the Continuous Cap Surface Concrete Model (MAT159) or the Riedel-Thoma-Hiermaier Concrete Model (MAT272), of which both demands more complex data input regarding the concrete material, MAT_072R3 does not seem to be able to exhibit the structural response of the beam model in the tests performed.

The above concern brings us to Mat_000-Add_Erosion. Concrete Damage Model Release 3 only exhibits the stress on each elements, but it does not allow failure and erosion [13]. This erosion model provides a way of including failure in the models. It is based on the concept that the concrete element is deleted when the material response in an element reaches a certain critical value [23]. In order to simulate the deletion of failed elements, the parameters MXEPS and EPSSH are studied. MXEPS stands for maximum principal strain at failure, wheareas EPSSH refers to the shear strain at failure. These two erosion criteria are considered to simulate material failure caused by crushing and spalling of concrete during impact (local failure) [17]. For a more accurate depiction of cracking patterns, the mesh of 3-5mm per element is required for the usage of this material model.

However, the required values for both parameters EPSSH and MXEPS of MAT_000-Add_Erosion can only be decided upon using trial and error method. Since after author has carried out the simulation study on this material card in order to achieve the correct deletion of elements in accordance to the validation beam model of Fujikake et al.'s [8] experiment, and has failed to simulate both the local failure at point of contact between the drop weight and the concrete beam (compression) and the flexural cracks at the bottom part of concrete beam under tension, the material card of erosion is not included for the parametric study. Regardless, the general trend of cracking pattern of the beam model can still be observed through the effective plastic strain illustration on LS-DYNA, even though it does not depict the actual failure mode of the beam.

3. METHODOLOGY

3.1 Validation of Base Model

Before commencing the beam modeling for the intended objective of this paper, the validation of the modeling of the beam on LS-DYNA with actual experimental results done by previous researches has been made to ensure that the beam model is functional. To achieve this purpose, the research work by Fujikake et al. [8] on the impact response of reinforced concrete beam has been chosen to perform the validation. This research is done by performing via Falling Weight Impact Loading Test, and it aims to develop an analytical model in order to predict the maximum deflection and the maximum impact load at the mid-span of a beam under impact loading, which ideally should match the experimental works done by Fujikake on his previous research.

For Fujikake et al.'s [8] experiment, 12 RC beam specimens are prepared, where all the beams have the same dimension of 150mmx250mmx1700mm (width, depth and length respectively). The 12 RC beams are divided into 3 groups: the first group of specimen is with reinforcement bars of D16 on both compression and tension side; the second group of specimen is reinforced with D13 bars at the compression side and D22 bars at the tension side; and the last group with D22 reinforcement bars at both compression and tension sides. The yield strengths of D13, D16 and D22 are 397MPa, 426MPa and 418MPa respectively. Each beam is made with 22 stirrups of D10 bars of strength 295 MPa spanning throughout the beam, spacing 75mm apart. The concrete compressive strength was given to be 42 MPa.

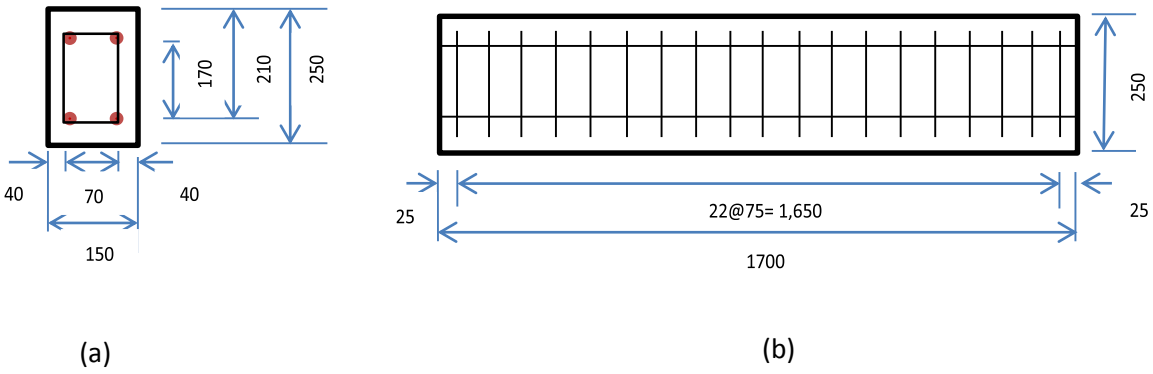

FIGURE 3.1.1. Arrangement of reinforcement bars: (a) Cross-sectional view; (b) longitudinal view, unit = mm

Designation	Number and Size (mm)	
	Compression Side	Tension Side
S1616	2D16	2D16
S1322	2D13	2D22
S2222	2D22	2D22

TABLE 3.1.1. Longitudinal bar arrangements.

In order to simulate the impact loading test, a sphere with mass of 400kg and a radius of 90mm (in accordance to the radius of the hemispherical tip of the drop hammer used in the experiment) is being dropped without any constrain (free-fall) onto the top surface of the mid-span of the beam model at different drop heights for each beam, which all are listed as below. The beam model is designed to be a simply-supported beam, of which bottom supports and top supports at both sides of the beams are provided. The top support is constrained of all movements (displacement at x, y, and z axis directions and rotation about x, y, and z axis) and the bottom supports are allowed to rotate about the x-axis but also are constrained in every other movements.

In LS-DYNA, the simulation is not able to take account of the free fall of the drop weight (that is with gravitational acceleration of g = 9.80665 m^2/s). Setting the drop height only affects the time between the initial position of the drop weight and the contact time of the drop weight with the top surface of the beam, without giving any increasing values towards the velocity. Therefore, the velocity of the drop weight at point of contact which includes the gravitational acceleration is calculated by using the formula: $V = \sqrt{2gh}$.

Drop Weight Test Height (m)	Equivalent Velocity of Drop Weight at Contact Point (m/s)
0.15	1.715
0.3	2.426
0.6	3.43
1.2	4.851
2.4	6.861

TABLE 3.1.2. Drop weight test heights to its respective velocity at contact point with the beam model.

The experimental beam specimen is modeled out in LS-DYNA using a mesh of 25mm. For the beam model's material properties, both reinforcement bars and the stirrups are tested as *Mat 003 Plastic Kinematic*, where all the data are taken to be as the properties of mild steel (Modulus of Elasticity = 210 GPa, mass density = 7850 kg/m^3). This material model is used to apply both the initial elastic data as well as the secondary plastic (post yield) portion of the stress-strain curve. The concrete body is subjected to *Mat 072R3-Concrete_Damage_REL3*. Duplicated nodes between the reinforcement bars, stirrups and the concrete are merged in order to signify a perfect bonding between all the materials. In order to simulate the cracking patterns, *Mat 000 Add Erosion* keyword is also studied.

3.2 Element Mesh Size Sensitivity Study

Mesh sensitivity study is carried out in order to study the effects of the meshing size of beam model in LS-DYNA on the behavior of the beams. The study is done by using the same validation model, albeit each beam specimens are modelled and analyzed repetitively using different mesh sizes of 25mm (default), 15mm, 12.5mm, 7.5mm and 5mm. The purpose of this mesh sensitivity study is to find the best element meshing size which gives the closest outcome to the experimental results.

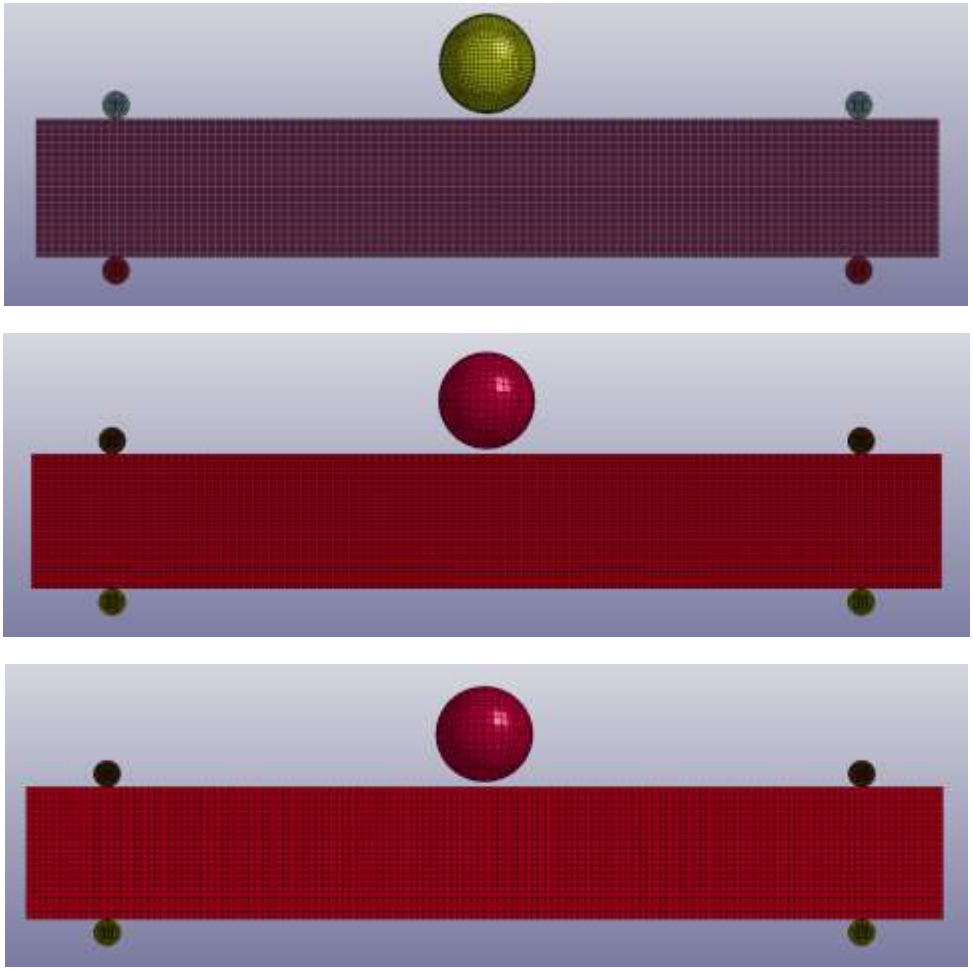

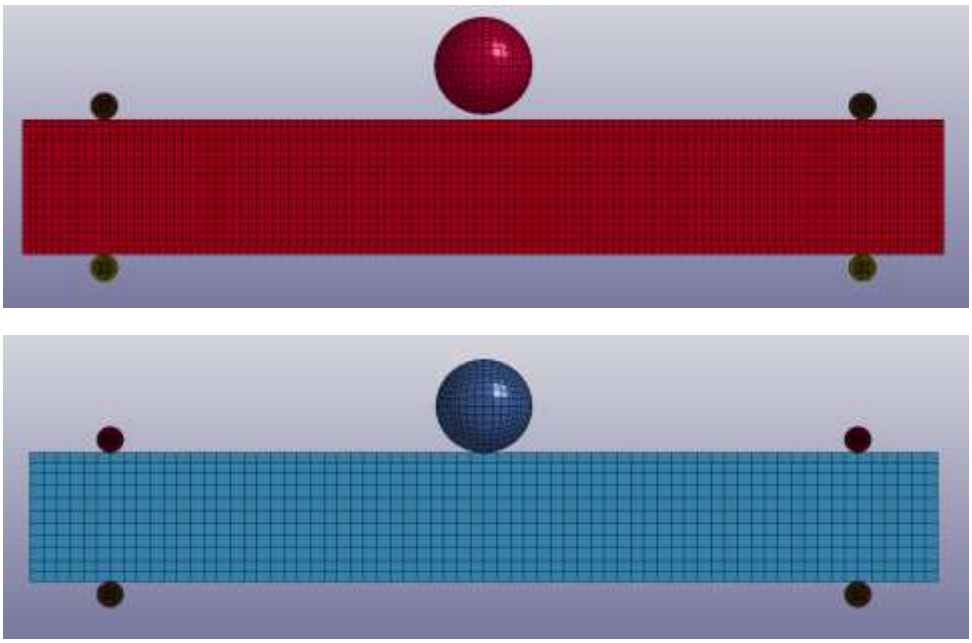

FIGURE 3.2.1. Beam model with meshing size of 5mm, 7.5mm, 12.5mm, 15mm and 25mm respectively.

0.15m	**Y-Displacement**	**% of Deviation**	**Resultant Force**	**% of Deviation**
5mm	5.04	18.80%	146.75	19.13%
7.5mm	5.17	16.79%	151.93	23.34%
12.5mm	5.21	16.12%	150.86	22.47%
15mm	5.37	13.56%	133.39	8.29%
25mm	5.67	8.80%	142.00	15.27%
Experiment	6.21		123.19	
0.3m				
5mm	8.81	21.34%	171.51	1.17%
7.5mm	9.31	16.93%	219.16	29.28%
12.5mm	9.55	14.80%	208.57	23.03%
15mm	9.56	14.68%	211.54	24.79%
25mm	10.26	8.38%	188.43	11.15%
Experiment	11.20		169.52	
0.6m				
5mm	17.04	15.34%	240.22	1.17%
7.5mm	17.73	11.92%	195.98	19.37%
12.5mm	17.89	11.12%	194.35	20.04%
15mm	18.81	6.54%	202.01	16.89%
25mm	19.25	4.35%	228.24	6.10%
Experiment	20.13		243.06	

1.2m				
5mm	34.47	6.65%	228.93	27.93%
7.5mm	36.33	1.64%	249.51	21.45%
12.5mm	37.77	2.27%	249.27	21.53%
15mm	39.44	6.80%	259.35	18.35%
25mm	39.07	5.79%	306.45	3.53%
Experiment	36.93		317.65	

TABLE 3.2.1. Computed maximum y-displacement at mid-span and resultant forces of all mesh sizes for beam specimens S1616 for drop heights 0.15m, 0.3m, 0.6m, and 1.2m.

As observed from the above table, at different drop heights, different meshing sizes seem to produce accurate results. However, in comparison with the other meshing sizes, the beam models with element mesh of 25mm appears to give a more stable result in terms of deflection, where the percentage of deviation are all less than 9%. As for the maximum impact forces, the beam models with 25mm element mesh, although does not produce the closest value to the experimental results, is also the most stable compared to other element meshing sizes, as it maintains to be lower than 16%. Therefore, the element meshing size of 25mm is used for the parametric study.

3.3 Parametric Study

After successfully validating the base model, the actual parametric study is ready to be started by using the exact same inputs as the base model.

For the parametric study, the cross section of the beam model is set to be a fixed dimension of 150mm width x 250mm depth, with two longitudinal reinforcement steel bars of diameters 16mm, 20mm, 22mm and 25mm (all with the same yield strength of 500MPa) at both tension and compression side. One part of the beam specimens are tested without any shear reinforcement, whereas another part of the beam specimens are shear-reinforced with steel bars of 6mm diameter and yield strength of 295 MPa, with a varying percentage of 0.1%, 0.2%, 0.3% and 0.4%. The cover of the link to the outer surface of beam is set to be a fixed 50mm for all specimens. The length of beam specimens vary depending on the a/d ratio, of which the values 2, 3, 4 and 5 will be tested. Concrete strength is set to be 30 MPa, with Poisson's ratio value of 0.02.

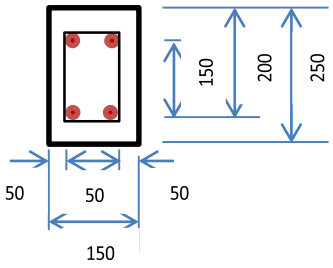

FIGURE 3.3. Details of the arrangement of reinforcement bars: Cross-sectional view, unit =mm

All the specimens are tested with the same velocity and same mass of drop weight, which are 6 m/s and 400 kg respectively. The aforementioned specifications of the beams are combined and done in different series, where each beam models have either different a/d ratio, main reinforcement percentage or shear reinforcement ratio (project activity as listed in chapter 3.4). There are a total of 60 beam models to be analyzed.

3.4 Project Activity

A project activity plan has been created in the form of excel spreadsheet before the parametric study starts for the ease of keeping track of progress.

The research is divided into 4 basic test series with different a/d ratio, each focusing on the effects of one parameter of interest on the dynamic behavior of the beam model.

	a/d				Main Reinforcement			Shear Reinforcement				
	2	3	4	5	1.34%	2.00%	3.00%	0.00%	0.10%	0.20%	0.30%	0.40%
					2T16	2T20	2T25	-	350 mm	175 mm	125 mm	95 mm
B02_16												
B02_16_350												
B02_16_175												
B02_16_125												
B02_16_95												
B02_20												
B02_20_350												
B02_20_175												
B02_20_125												
B02_20_95												
B02_25												
B02_25_350												
B02_25_175												
B02_25_125												
B02_25_95												

	a/d				Main Reinforcement			Shear Reinforcement				
	2	3	4	5	1.25%	2.00%	3.00%	0.00%	0.10%	0.20%	0.30%	0.40%
					2T16	2T20	2T25	-	350 mm	175 mm	125 mm	95 mm
B03_16												
B03_16_350												
B03_16_175												
B03_16_125												
B03_16_95												
B03_20												
B03_20_350												
B03_20_175												
B03_20_125												
B03_20_95												
B03_25												
B03_25_350												
B03_25_175												
B03_25_125												
B03_25_95												

	a/d				Main Reinforcement			Shear Reinforcement				
	2	3	4	5	1.25%	2.00%	3.00%	0.00%	0.10%	0.20%	0.30%	0.40%
					2T16	2T20	2T25	-	350 mm	175 mm	125 mm	95 mm
B04_16												
B04_16_350												
B04_16_175												
B04_16_125												
B04_16_95												
B04_20												
B04_20_350												
B04_20_175												
B04_20_125												
B04_20_95												
B04_25												
B04_25_350												
B04_25_175												
B04_25_125												
B04_25_95												

	a/d				Main Reinforcement			Shear Reinforcement				
	2	3	4	5	1.25%	2.00%	3.00%	0.00%	0.10%	0.20%	0.30%	0.40%
					2T16	2T20	2T25	-	350 mm	175 mm	125 mm	95 mm
B05_16												
B05_16_350												
B05_16_175												
B05_16_125												
B05_16_95												
B05_20												
B05_20_350												
B05_20_175												
B05_20_125												
B05_20_95												
B05_25												
B05_25_350												
B05_25_175												
B05_25_125												
B05_25_95												

TABLE 3.4. Project activity plan inclusive of all the parameters of interest, including the a/d ratio, the longitudinal reinforcement ratio and the shear reinforcement ratio.

4. RESULTS AND DISCUSSIONS

The simulation is done for the all the beams as listed in the project activity plan. Below are a comparison of results for different parameters:

4.1 Longitudinal reinforcement ratio

4.1.1 Without Shear Reinforcements

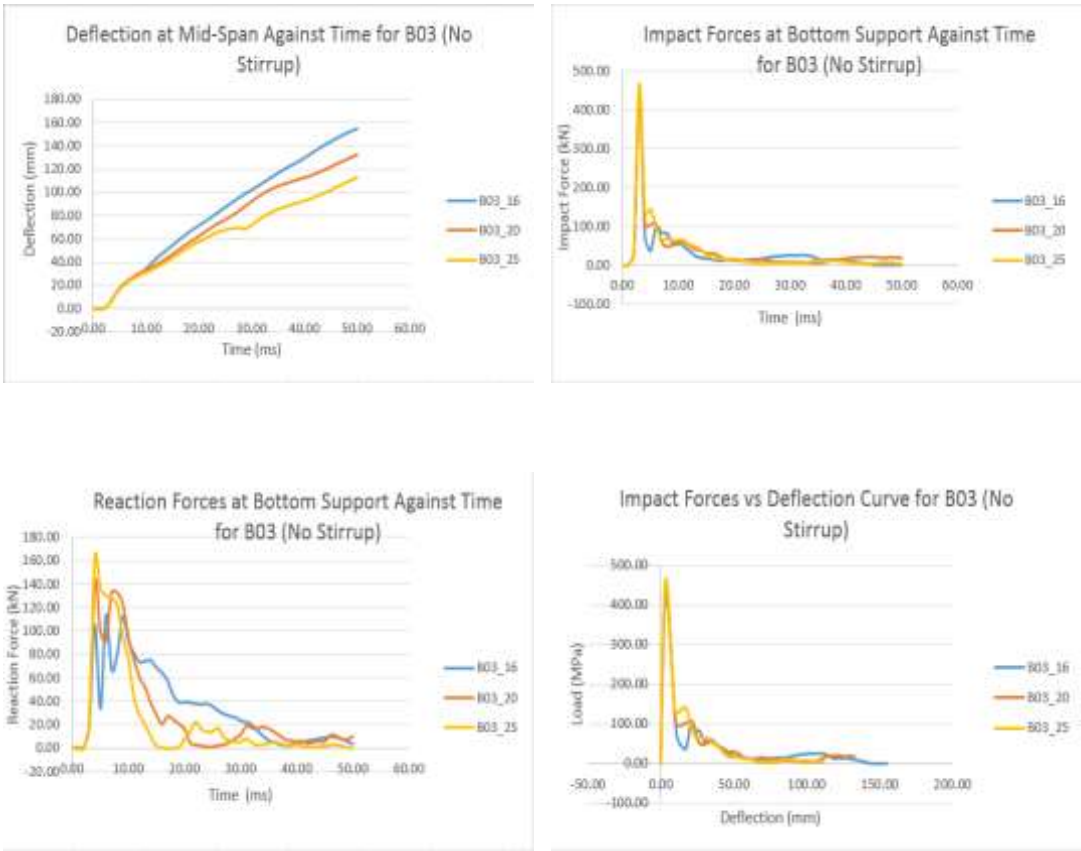

FIGURE 4.1.1. Graphs of the impact responses exhibited with respect to longitudinal reinforcement ratio by the beam models with a/d ratio = 3 and without shear reinforcement.

Rebar Size (mm)	Max. Deflection(mm)	Max. Reaction Force (kN)	Max. Impact Force (kN)
16	154.71	113.38	432.82
20	132.62	142.29	446.38
25	112.02	163.81	465.73

TABLE 4.1.1. Tabulated impact responses exhibited with respect to longitudinal reinforcement ratio by the beam models with a/d ratio = 3 and without shear reinforcement.

4.1.2 Shear Reinforcement Ratio = 0.3%

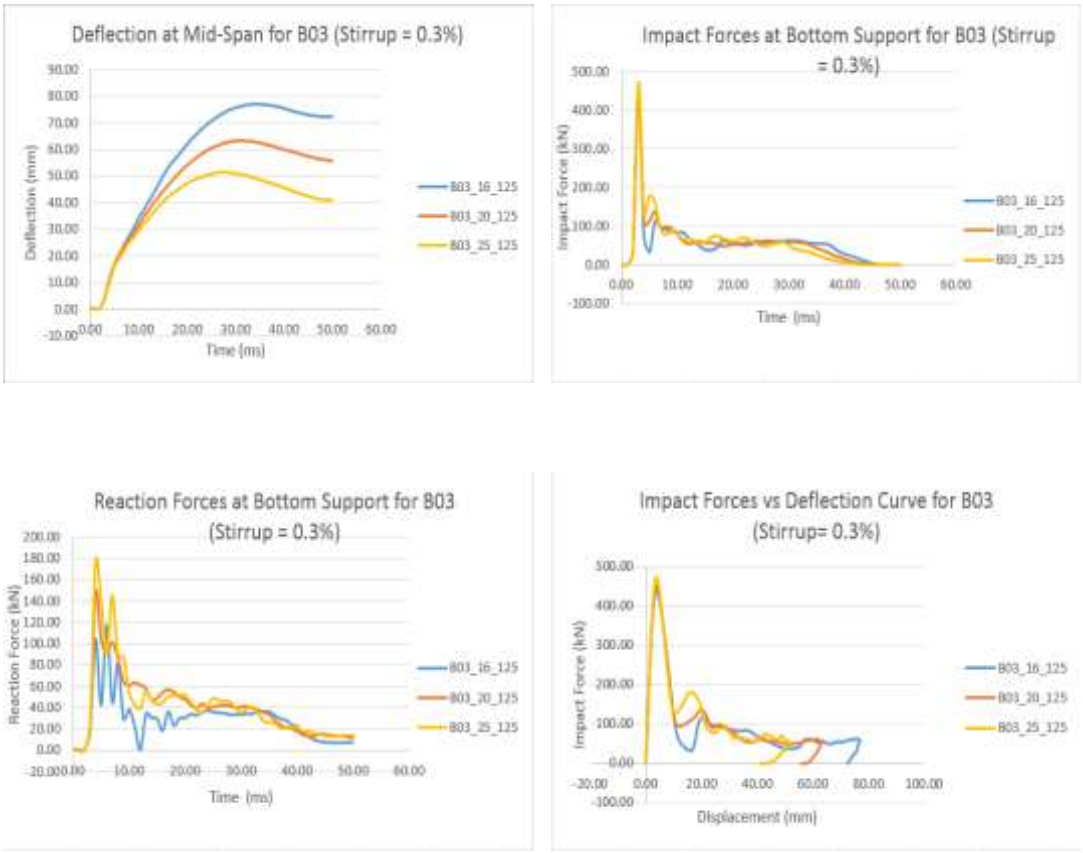

FIGURE 4.1.2. Graphs of the impact responses exhibited with respect to longitudinal reinforcement ratio by the beam models with a/d ratio = 3 and shear reinforcement of ratio = 0.3%.

Rebar Size (mm)	Max. Deflection (kN)	Max. Reaction Force (kN)	Max. Impact Force (kN)
16	76.98	117.51	438.08
20	63.53	148.41	453.02
25	51.51	176.08	472.90

TABLE 4.1.2. Tabulated impact responses exhibited with respect to longitudinal reinforcement ratio by the beam models with a/d ratio = 3 and with shear reinforcement of ratio =0.3%.

4.1.3 Shear Reinforcement Ratio = 0.4%

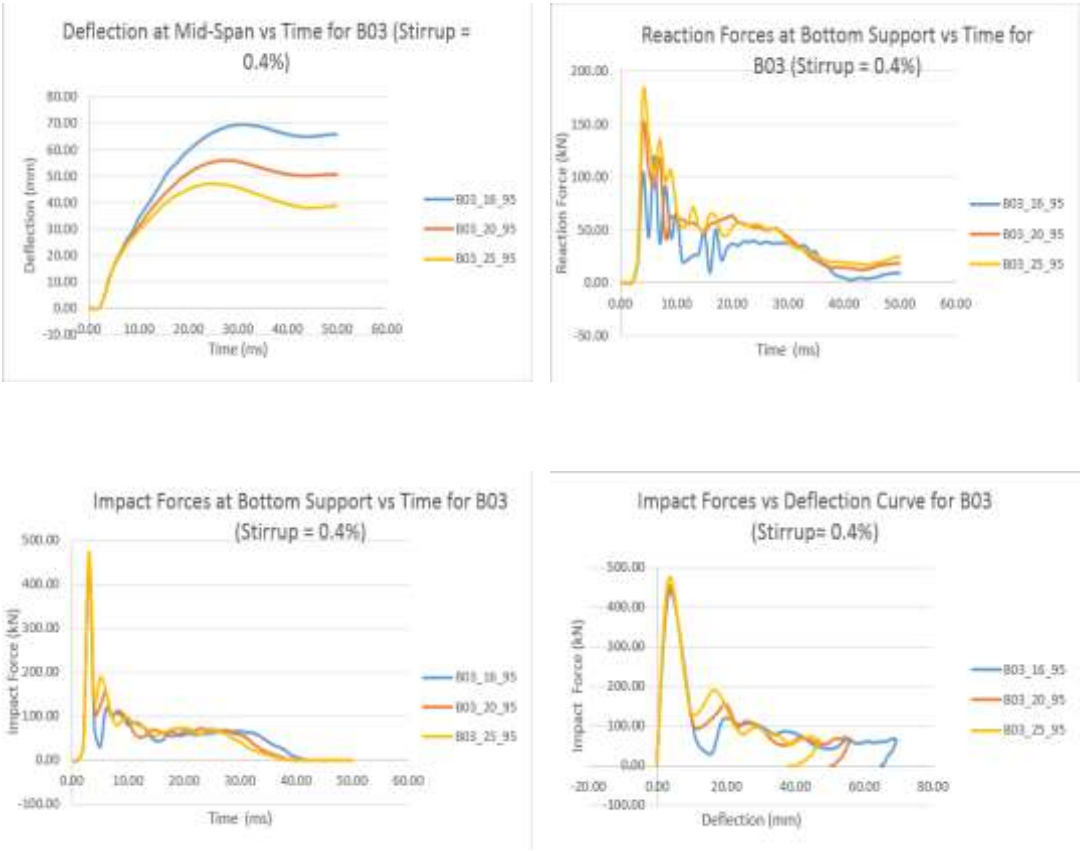

FIGURE 4.1.3. Graphs of the impact responses exhibited with respect to longitudinal reinforcement ratio by the beam models with a/d ratio = 3 and shear reinforcement of ratio = 0.4%.

Rebar Size (mm)	Max. Deflection (kN)	Max. Reaction Force (kN)	Max. Impact Force (kN)
16	69.50	119.88	440.45
20	56.00	149.49	455.43
25	47.26	180.51	474.99

TABLE 4.1.3. Tabulated impact responses exhibited with respect to longitudinal reinforcement ratio by the beam models with a/d ratio = 3 and with shear reinforcement of ratio =0.4%.

Among the outcomes checked are the mid-span deflection, impact force at point of contact between the drop weight and the surface of beam model and the reaction forces at both bottom supports.

In terms of impact forces at point of contact between drop weight and the surface of beam model, the beams were found to fail at higher loads with the increase in the longitudinal reinforcement ratio, signifying that there is an increase in load carrying capacity in the beam. This reaction is in lieu with what Banthia and Mindesss and et. Al mentioned [7] [1] [2] [8] mentioned, that concrete beams show higher impact strength and higher fracture energies at higher stressing rates.

As for the maximum vertical displacement, it was as predicted to decrease when the longitudinal reinforcement ratio increase. However, the more interesting part of finding is that, even though the mass of drop weight and drop velocity remains the same, the reaction forces at the bottom supports increases as the rebar size increases, which is different from the behavior of beams applied with static load, where the sum of reaction forces should equal the load applied to the structural member.

4.2 Shear reinforcement ratio

4.2.1 a/d Ratio = 2

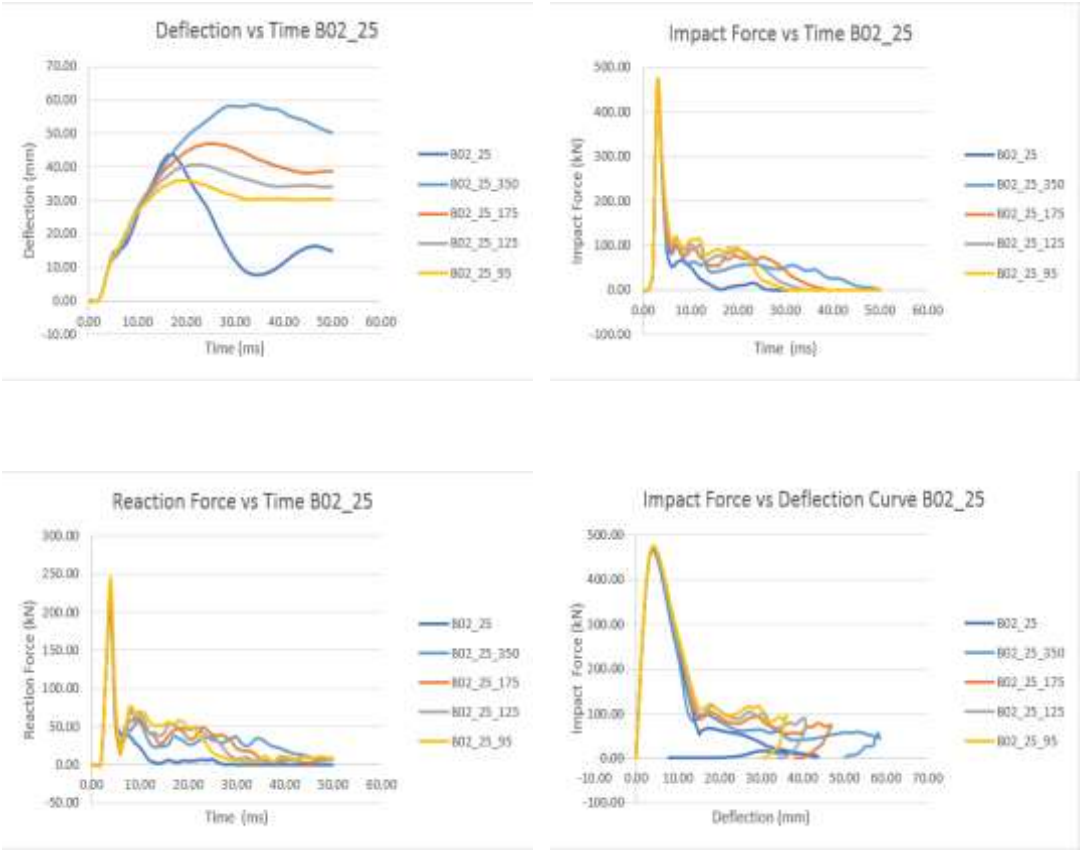

FIGURE 4.2.1. Graphs of the impact responses in respect to shear reinforcement ratio exhibited by the beam models with a/d ratio = 2 and with main reinforcements of 2T25.

Stirrup Ratio (%)	Max. Deflection(mm)	Max. Reaction Force (kN)	Max. Impact Force (kN)
0	43.74	203.75	460.88
0.1	58.66	218.27	461.16
0.2	46.93	229.38	467.07
0.3	40.63	235.13	467.56
0.4	36.03	244.42	469.34

TABLE 4.2.1. Tabulated impact responses in respect to shear reinforcement ratio exhibited by the beam models with a/d ratio = 2 and with main reinforcements of 2T25.

4.2.2 a/d Ratio = 3

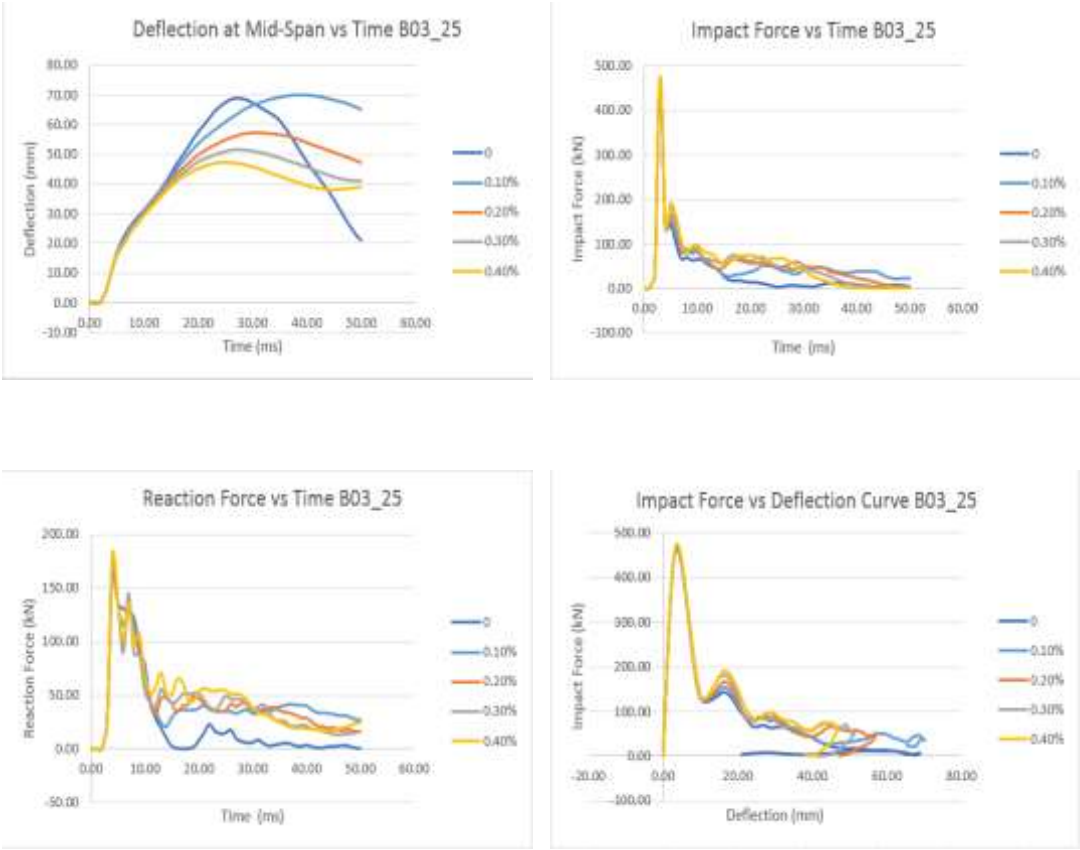

FIGURE 4.2.2. Graphs of the impact responses in respect to shear reinforcement ratio exhibited by the beam models with a/d ratio = 3 and with main reinforcements of 2T25.

Stirrup Ratio (%)	Max. Deflection(mm)	Max. Reaction Force (kN)	Max. Reaction Force (kN)
0	68.99	163.81	465.73
0.1	70.16	169.20	471.92
0.2	57.23	174.33	472.71
0.3	51.51	176.08	472.90
0.4	47.26	180.51	474.99

TABLE 4.2.2. Tabulated impact responses in respect to shear reinforcement ratio exhibited by the beam models with a/d ratio = 3 and with main reinforcements of 2T25.

4.2.3 a/d Ratio = 4

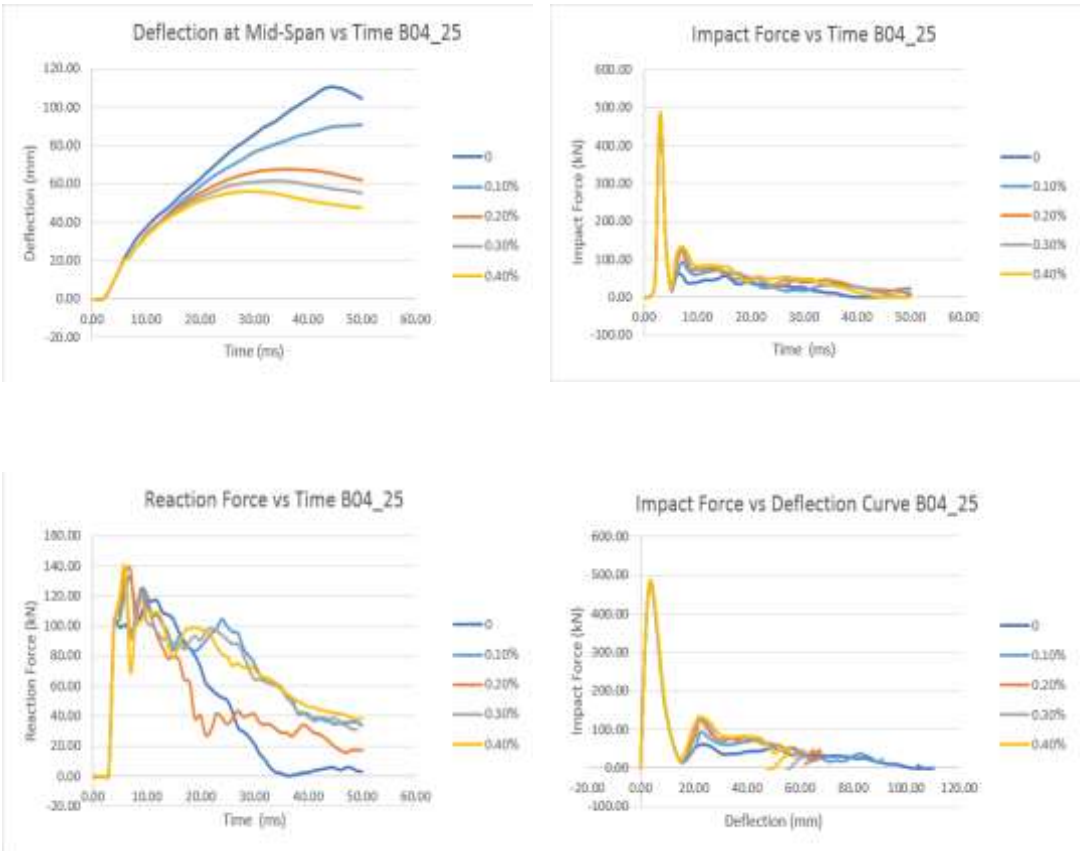

FIGURE 4.2.3. Graphs of the impact responses in respect to shear reinforcement ratio exhibited by the beam models with a/d ratio = 4 and with main reinforcements of 2T25.

Stirrup Ratio (%)	Max. Deflection(mm)	Max. Reaction Force (kN)	Max. Reaction Force (kN)
0	110.39	116.88	477.30
0.1	90.97	133.35	477.59
0.2	67.53	138.58	484.21
0.3	61.71	138.27	485.34
0.4	56.22	138.61	487.30

TABLE 4.2.3. Tabulated impact responses in respect to shear reinforcement ratio exhibited by the beam models with a/d ratio = 4 and with main reinforcements of 2T25.

4.2.4 a/d Ratio = 5

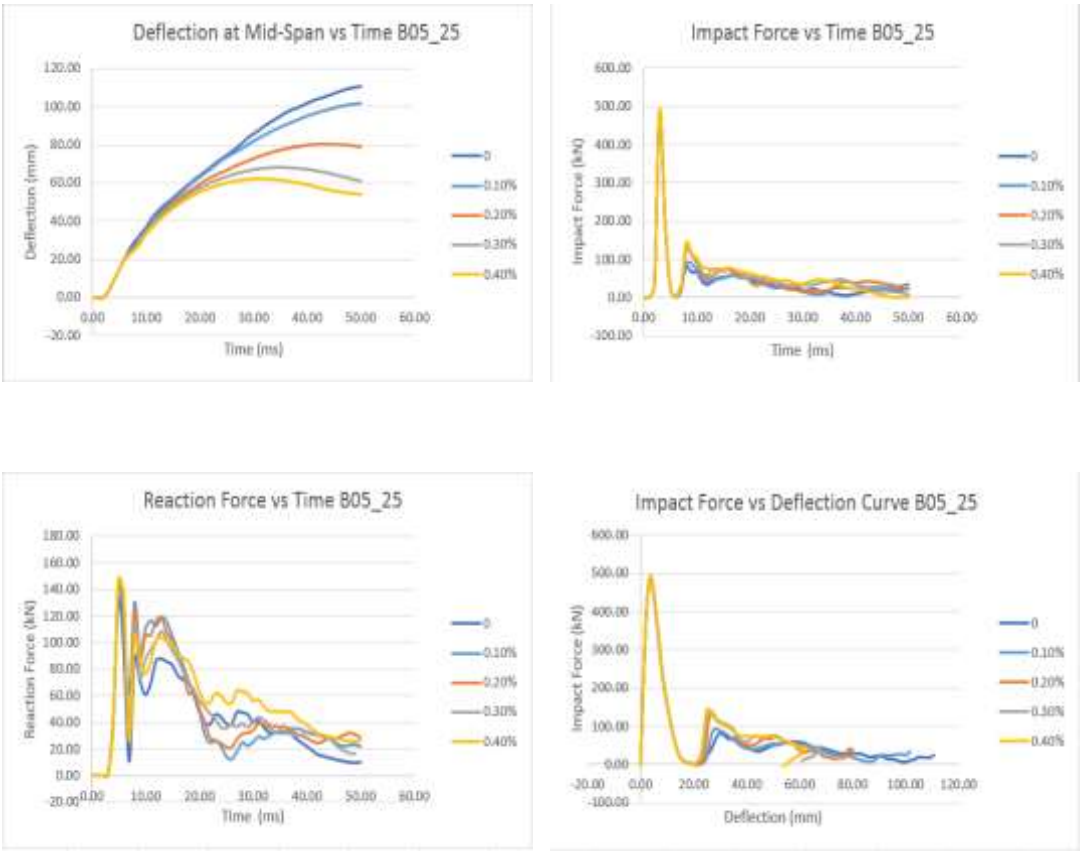

FIGURE 4.2.4. Graphs of the impact responses in respect to shear reinforcement ratio exhibited by the beam models with a/d ratio = 5 and with main reinforcements of 2T25.

Stirrup Ratio (%)	Max. Deflection(mm)	Max. Reaction Force (kN)	Max. Reaction Force (kN)
0	110.80	132.21	481.50
0.1	101.56	141.83	487.82
0.2	80.08	146.00	488.23
0.3	67.98	146.76	489.28
0.4	62.07	148.30	491.35

TABLE 4.2.4. Tabulated impact responses in respect to shear reinforcement ratio exhibited by the beam models with a/d ratio = 5 and with main reinforcements of 2T25.

For the parameter of varying shear reinforcement ratio, beam models with higher shear reinforcements have higher impact resistance force, similar to the behavior of increasing longitudinal reinforcement ratios and agreeing with Saatci and Vecchio [22], but the increase in the impact resistance force is not that significant.

As for the maximum deflection, with the increase of shear reinforcement ratio, there is a decrease in the maximum deflection value. However, for graphs with shear reinforcement ratio = 0, it can be seen that there is a sharp drop after the beam reaches its maximum deflection. This is due to the limitation of the material card that is used to model out the concrete damage, which is MAT 072. When the material reaches a state where it totally fails, instead of performing element deletions, the material card will enable the model to go into a softening response, of which the model becomes unstable.

In terms of reaction forces, it can be observed that with an increase in shear reinforcement ratio, there is an increase in maximum reaction forces at the bottom supports, meaning that the additional stirrups can actually help in the transfer of impact forces experienced by the beam model to the bottom supports.

4.3 a/d Ratio

4.3.1 without shear reinforcement

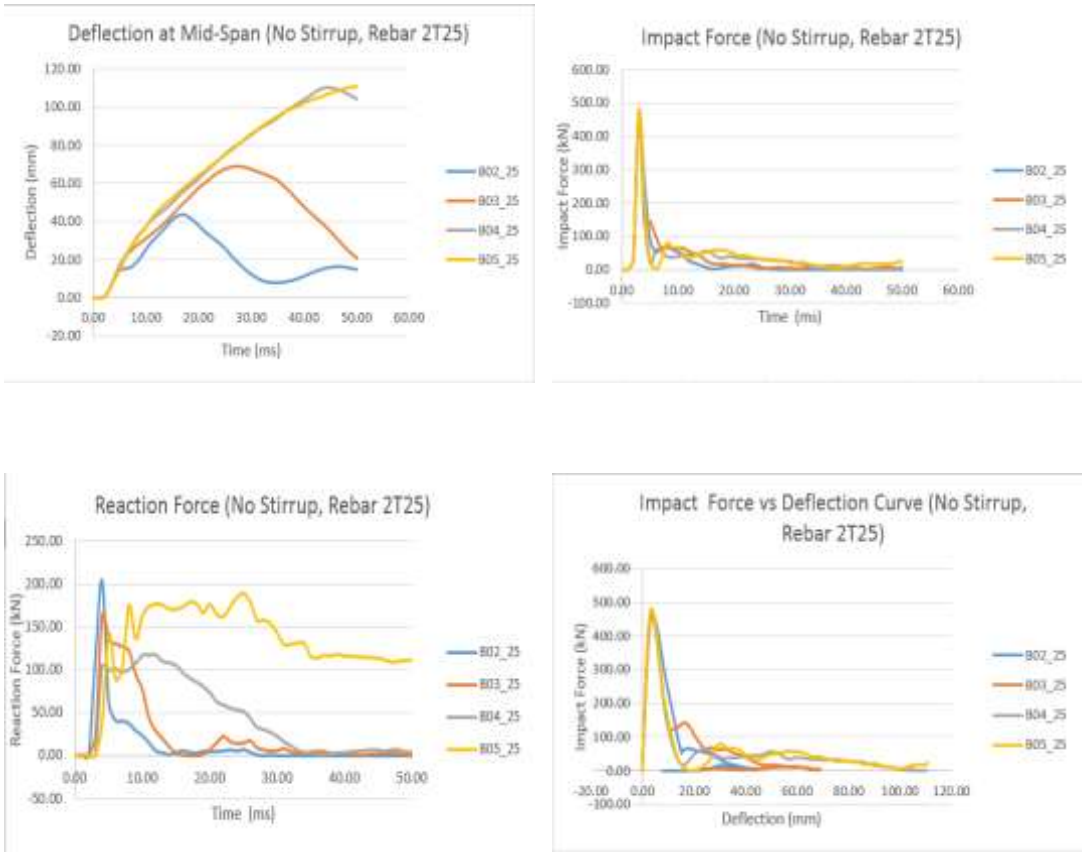

FIGURE 4.3.1. Graphs of the impact responses in respect to a/d ratio exhibited by the beam models without shear reinforcements and with main reinforcements of 2T25.

a/d ratio	Max Deflection (mm)	Max. Reaction Force (kN)	Max. Impact Force (kN)
2	43.74	203.75	460.88
3	68.99	163.81	465.73
4	110.39	116.88	477.30
5	110.80	189.08	481.50

TABLE 4.3.1. Tabulated impact responses in respect to a/d ratio exhibited by the beam models without shear reinforcements and with main reinforcements of 2T25.

4.3.2 Shear Reinforcement Ratio = 0.1%

FIGURE 4.3.2. Graphs of the impact responses in respect to a/d ratio exhibited by the beam models with shear reinforcement of ratio = 0.1% and with main reinforcements of 2T25.

a/d ratio	Max Deflection (mm)	Max. Reaction Force (kN)	Max. Impact Force (kN)
2	58.66	218.27	461.16
3	70.16	169.20	471.92
4	90.97	133.35	477.59
5	101.56	132.79	487.82

TABLE 4.3.2. Tabulated impact responses in respect to a/d ratio exhibited by the beam models with shear reinforcement of ratio = 0.1% and with main reinforcements of 2T25.

4.3.3 Shear Reinforcement Ratio = 0.2%

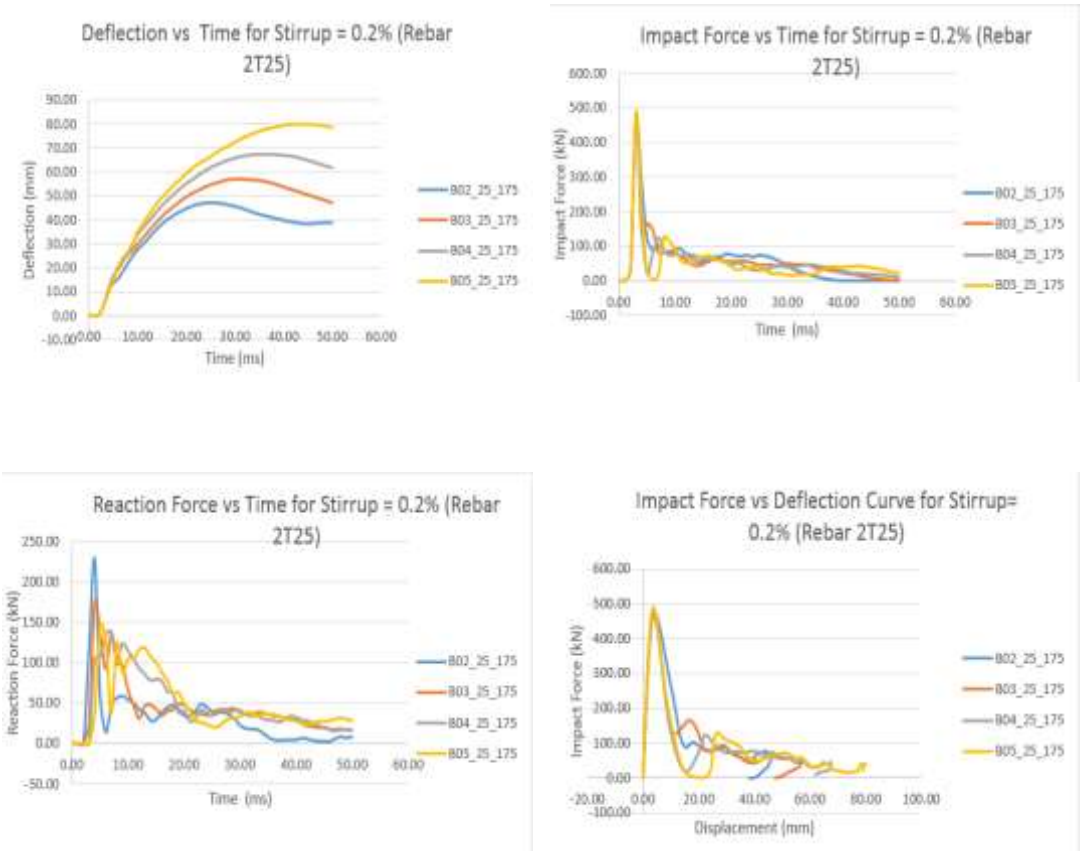

FIGURE 4.3.3. Graphs of the impact responses in respect to a/d ratio exhibited by the beam models with shear reinforcement of ratio = 0.2% and with main reinforcements of 2T25.

a/d ratio	Max Deflection (mm)	Max. Reaction Force (kN)	Max. Impact Force (kN)
2	46.93	229.38	467.07
3	57.23	174.33	472.71
4	67.53	138.58	484.21
5	80.08	146.00	488.23

TABLE 4.3.3. Tabulated impact responses in respect to a/d ratio exhibited by the beam models with shear reinforcement of ratio = 0.2% and with main reinforcements of 2T25.

4.3.4 Shear Reinforcement Ratio = 0.3%

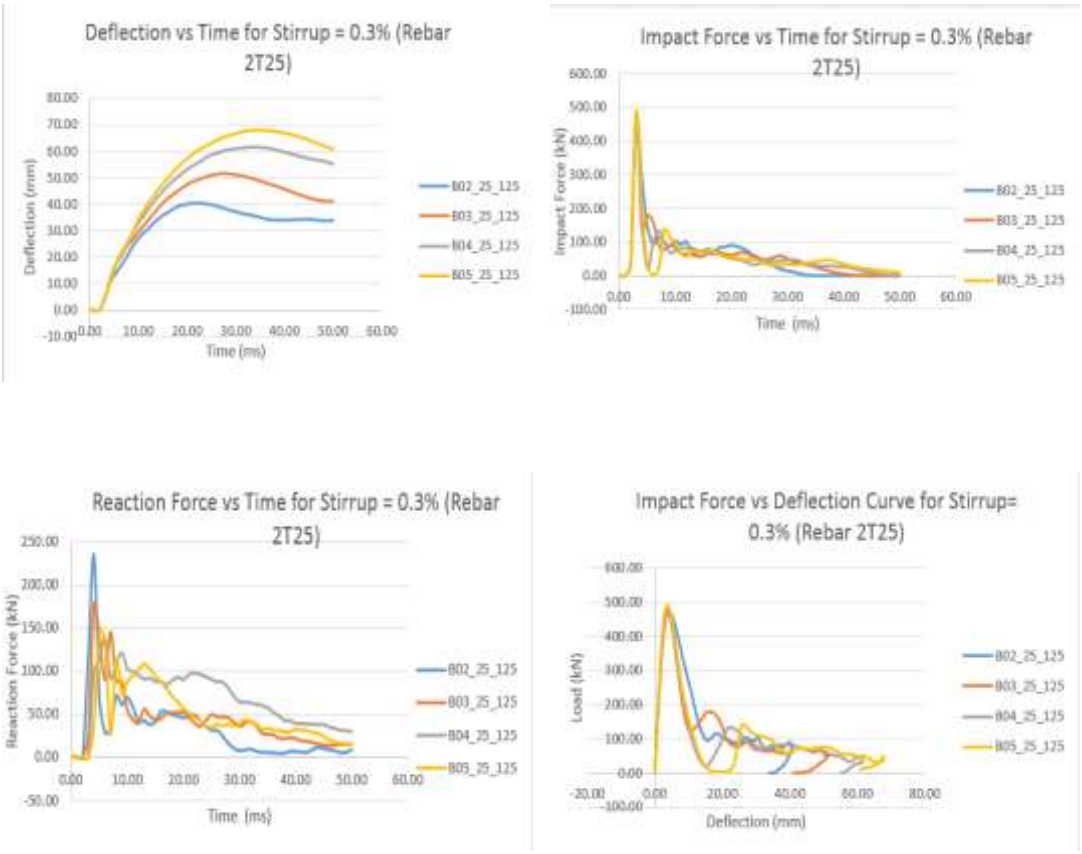

FIGURE 4.3.4. Graphs of the impact responses in respect to a/d ratio exhibited by the beam models with shear reinforcement of ratio = 0.3% and with main reinforcements of 2T25.

a/d ratio	Max Deflection (mm)	Max. Reaction Force (kN)	Max. Impact Force (kN)
2	40.63	235.13	467.56
3	51.51	176.08	472.90
4	61.71	138.27	485.34
5	67.98	146.76	489.28

TABLE 4.3.4. Tabulated impact responses in respect to a/d ratio exhibited by the beam models with shear reinforcement of ratio = 0.3% and with main reinforcements of 2T25.

4.3.5 Shear Reinforcement Ratio = 0.4%

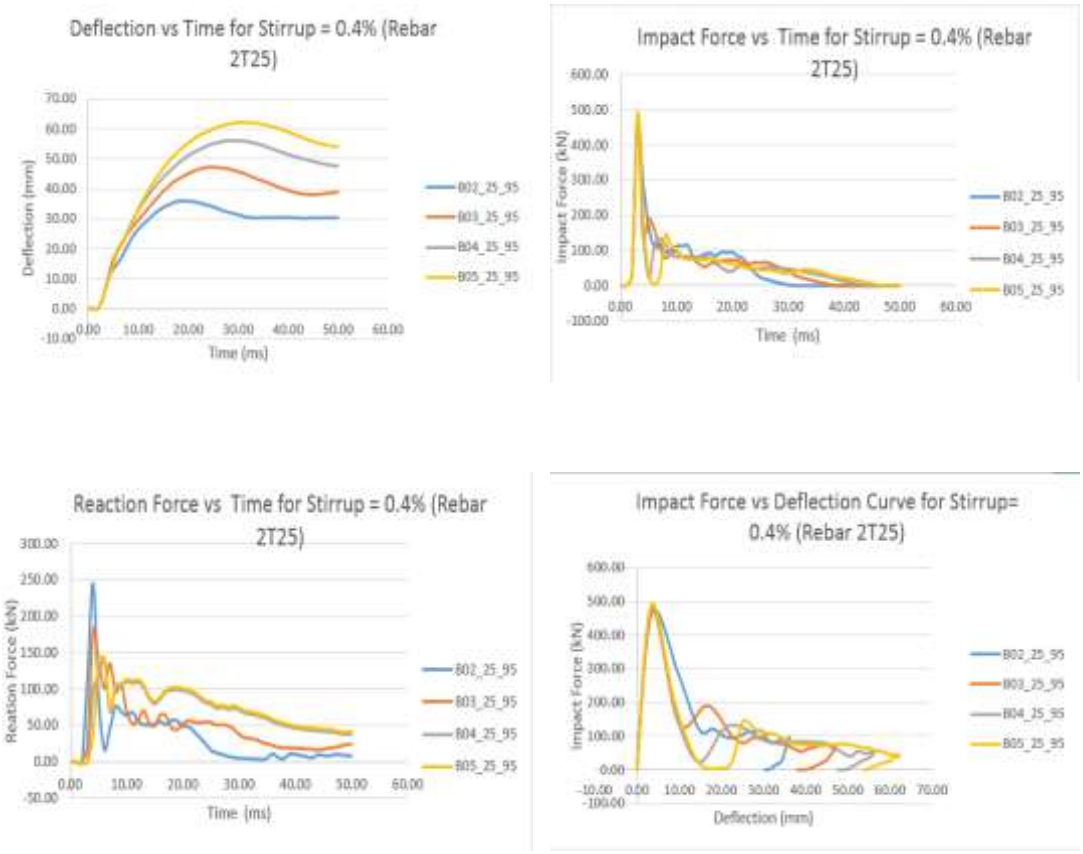

FIGURE 4.3.5. Graphs of the impact responses in respect to a/d ratio exhibited by the beam models with shear reinforcement of ratio = 0.4% and with main reinforcements of 2T25.

a/d ratio	Max Deflection (mm)	Max. Reaction Force (kN)	Max. Impact Force (kN)
2	36.03	244.42	469.3
3	47.26	180.51	475.0
4	56.22	138.61	487.3
5	62.07	141.95	491.4

TABLE 4.3.5. Tabulated impact responses in respect to a/d ratio exhibited by the beam models with shear reinforcement of ratio = 0.4% and with main reinforcements of 2T25.

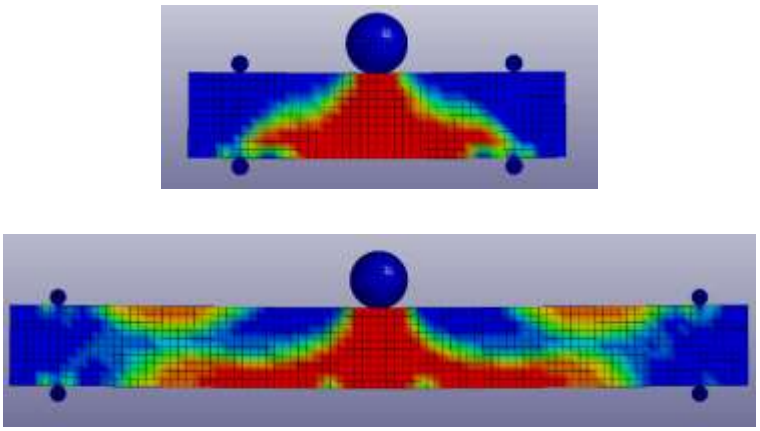

FIGURE 4.3.6. Plot of effective strain distribution in LS-DYNA for beam models with a/d ratio = 2 and 5 respectively.

In terms of the shear span-to-depth ratio, it appears that with an increase in a/d ratio, the tensile stresses experienced in the beam does not reach the support. The area of tensile stresses has increased relatively, but the distance between the end of tensile stresses when it reaches the bottom surface of beam and the bottom support are getting further apart. This phenomenon was also observed by Sharma and Ozbolt [11], whom deduced that it is due to intial forces caused by the high loading rate.

Besides, in static behavior, usually beams with low a/d ratio especially with ratio of 2 and lower will fail in shear, and the ones with higher ratio tend to fail in flexure. However, as observed from the figure above, the beam with a/d ratio of 2 seems to potentially fail in flexure, whereas the one with a/d ratio of 5 apparently has the potential to fail in either flexure or shear-compression mode. However, this visual observation might not be able to depict the actual failure mode of the beam. This is because even though MAT 072 is good in describing the material responses, but it does not seem to be able to reproduce structural responses, but requires additional material cards such as Mat Add Erosion.

In the graphs of reaction forces against time, it is apparent that for beams without shear reinforcements, there is not much difference in terms of reaction forces

at the bottom supports in cases with different a/d ratio, but as shear reinforcements are added in, there is s a major increase in the reaction forces at the bottom supports with the increase of a/d ratio.

5. CONCLUSION AND RECOMMENDATION

In conclusion, a parametric study has been done for reinforcement concrete beams subjected to impact loading via simulation by using the non-linear finite element analysis software LS-DYNA. The parameters tested including variation of longitudinal reinforcement ratio, shear reinforcement ratio and aspect (a/d) ratio. The simulation was done by performing a Falling Weight Impact Loading Test, where a drop weight of 400 kg is to fell without any contraints (free fall) unto the mid-span of a simply-supported beam, of which has a cross-section of 150mm width to 250 mm depth.

The project was first commenced by validating the base beam model for simulation with the experimental work of Fujikake et al.'s [8] paper. This is to ensure that the beam models have the correct input that can generate the same responses as if it is tested in an actual physical experiment. After making sure that the results match their experimental works, an element mesh size sensitivity test was carried out in order to find the best element mesh size that produces the best results in acccordance to the experimental ones. After confirming with the element mesh size of 25mm for the beam model, author was able to move on to the parametric study.

From the results, it can be concluded that with an increase in longitudinal reinforcement ratio and shear reinforcement ratio, there is an increase in impact resistance forces of the beam models, meaning that the beams have a higher load-carrying capacity. The variation of a/d ratio does not seem to have much effect on the maximum impact forces. The increase in longitudinal reinforcement ratio and shear reinforcement ratio has predictably decreased the maximum deflection experienced by the beam model, which increases as the a/d ratio of the beam model increases.

The reaction forces at the bottom supports of the beam models seemingly increases with the increase of longitudinal reinforcement ratio and shear reinforcement ratio, even when the mass of drop weight and the drop velocity is fixed throughout the

whole experiment. However, in the case of increasing a/d ratio, the reaction forces experienced at the bottom supports decreases, as the tensile stresses experienced by the beam does not reach the support due to iniertial forces. The failure mode of beams with varying a/d ratio for dynamic cases is an interesting aspect to check on, but due to the limitations of the material card used to simulate the concrete damage of the model, author was not able to confirm the beam models'failure modes.

The dynamic behavior of reinforced concrete beam is vastly different from the ones subjected to static loading. By performing this parametric study, the structural engineering community can hopefully have a better understanding on the way reinforced concrete beams behave when subjected to impact loading. Plus, there are so many potentials that can be done using the findings of the research, especially to validate the emperical formulas generated by the other researchers to predict the dynamic behavior of reinforced concrete members, to modify them or even come up with a new one based on these findings. This can be very beneficial, not only to the structural engineering community, but also the public by making a structure safer.

REFERENCE

[1] A. Miyamoto, M. E. King, and M. Fujii, "Non-linear Dynamic Analysis and Design Concepts for RC Beams Under Impulsive Loads," *New Zealand Nat. Soc. Earthquake Eng. Bull.,* pp. 98-111, 1989.

[2] D. M. Cotsovos, "A simplified approach for assessing the load-carrying capacity of reinforced concrete beams under concentrated load applied at high rates," *International Journal of Impact Engineering,* vol. 37, pp. 907-917, 8// 2010.

[3] B. Mosley, J. Bungey, and R. Hulse, *Reinforced Concrete Design to Eurocode 2*, 7 ed. UK: Palgrave Macmillan, 2012.

[4] N. Kishi and H. Mikami, "Empirical Formulas for Designing Reinforced Concrete Beams under Impact Loading," *Structural Journal,* vol. 109, 7/1/2012 2012.

[5] S. D. Adhikary, B. Li, and K. Fujikake, "Dynamic behavior of reinforced concrete beams under varying rates of concentrated loading," *International Journal of Impact Engineering,* vol. 47, pp. 24-38, 9// 2012.

[6] N. Kishi and A. Q. Bhatti, "An equivalent fracture energy concept for nonlinear dynamic response analysis of prototype RC girders subjected to falling-weight impact loading," *International Journal of Impact Engineering,* vol. 37, pp. 103-113, 1// 2010.

[7] N. P. Banthia, S. Mindess, and A. Bentur, "Impact behaviour of concrete beams," *Materials and Structures,* vol. 20, pp. 293-302, 1987/07/01 1987.

[8] K. Fujikake, B. Li, and S. Soeun, "Impact Response of Reinforced Concrete Beam and Its Analytical Evaluation," *Journal of Structural Engineering,* vol. 135, pp. 938-950, 2009/08/01 2009.

[9] H. Jiang, X. Wang, and S. He, "Numerical simulation of impact tests on reinforced concrete beams," *Materials & Design,* vol. 39, pp. 111-120, 8// 2012.

[10] M. E. Perdomo, R. Picón, M. E. Marante, F. Hild, S. Roux, and J. Flórez-López, "Experimental analysis and mathematical modeling of fracture in RC elements with any aspect ratio," *Engineering Structures,* vol. 46, pp. 407-416, 1// 2013.

[11] A. Sharma and J. Ožbolt, "Influence of high loading rates on behavior of reinforced concrete beams with different aspect ratios – A numerical study," *Engineering Structures,* vol. 79, pp. 297-308, 11/15/ 2014.

[12] J. Ožbolt and A. Sharma, "Numerical simulation of reinforced concrete beams with different shear reinforcements under dynamic impact loads," *International Journal of Impact Engineering*, vol. 38, pp. 940-950, 12// 2011.

[13] L. S. T. Corporation, "LS-Dyna Keyword User's Manual," *Material Models*, vol. II, 2014.

[14] D. M. Cotsovos and M. N. Pavlović, "Modelling of RC beams under impact loading," *Proceedings of the Institution of Civil Engineers - Structures and Buildings*, vol. 165, pp. 77-94, 2012.

[15] V. Gyliene and V. Ostasevicius, "Cowper-Symonds material deformation law application in material cutting process using LS-DYNA FE code: turning and milling," in *8th European LS-DYNA Users' Conference*.

[16] M. C. Jaime, "Numerical modeling of rock cutting and its associated fragmentation process using the Finite Element Method," 2012.

[17] M. A. K. M. Madurapperuma and A. C. Wijeyewickrema, "Columns in Reinforced Concrete Buildings Impacted by Tsunami Water-Borne Massive Objects," 2012.

[18] L. J. Malvar and C. A. Ross, "Review of Strain Rate Effects for Concrete in Tension," *Materials Journal*, vol. 95, 11/1/1998 1998.

[19] J. K. Paik and A. K. Thayamballi, *Ultimate Limit State Design of Steel-Plated Structures*: John Wiley & Sons, 2003.

[20] G. S. H. Samir A. Ashour and F. W. Faisal, "Shear Behavior of High-Strength Fiber Reinforced Concrete Beams," *Structural Journal*, vol. 89, 3/1/1992 1992.

[21] L. E. Schwer and L. J. Malvar, "Simplified concrete modeling with *Mat_Concrete_Damage_Rel3," 2005.

[22] S. Saatci and J. F. Vecchio, "Effects of Shear Mechanisms on Impact Behavior of Reinforced Concrete Beams," *Structural Journal*, vol. 106, 1/1/2009 2009.

[23] G. Thiagarajan, A. V. Kadambi, S. Robert, and C. F. Johnson, "Experimental and finite element analysis of doubly reinforced concrete slabs subjected to blast loads," *International Journal of Impact Engineering*, vol. 75, pp. 162-173, 1// 2015.